REMOTE SENSING ANALYSES OF SMALL TERRESTRIAL VOLCANIC AND IMPACT CRATERS: A MARS ANALOG FOR FORMATION, MORPHOLOGY, AND EROSIONAL PROCESSES. V. M. Peet[1], M. S. Ramsey[1], and D. A. Crown[2], [1]Department of Geology and Planetary Science, University of Pittsburgh, Pittsburgh, PA 15260, vmp10@pitt.edu, ramsey@ivis.eps.pitt.edu, [2]Planetary Science Institute, 1700 E. Ft. Lowell Rd., Suite 106, Tucson, AZ 85719, crown@psi.edu.

Introduction: El Elegante Crater, a maar crater in the Pinacate Volcanic Field (PVF) in north-central Mexico, and Meteor Crater, an impact crater located in central Arizona, are the focus of an ongoing Mars analog study due to their similarity in size, morphology, age, and weathering history [1-2]. The purpose of this phase of the research is to isolate and quantify formation and subsequent sediment transport processes for terrestrial small craters using remote sensing datasets. The remote sensing datasets selected for this study are similar to those currently available for Mars [2]. Previously-reported field studies have been an integral factor in validating remote data and establishing techniques applicable to Mars.

Small craters may represent some of the most recent geologic activity on Mars [3]. Therefore, quantifying and differentiating formation and modification processes may have implications toward understanding climate and surface evolution. This work has direct implications for determining the presence and role of volatiles in Martian cratering processes with the development of techniques for distinguishing maar-like volcanoes from small impacts.

Background: El Elegante Crater formed ~32,000 years ago from explosive phreatomagmatic activity [4-6]. Meteor Crater formed ~50,000 years ago from the impact of an iron nickel meteorite [7]. Both of these craters appear as bowl-shaped, nearly-circular depressions with similar diameters and an annulus of ejecta that has been affected by weathering [4-7]. Ejecta topography and subsequent transport has been the focus of previous remote sensing work at Meteor Crater [8], which included lithologic unit mapping using linear deconvolution of thermal infrared (TIR) data of various resolutions [9-10].

For the current study, data collection and field observations were conducted at each crater in 2004. Equipment used included a real-time differential GPS (d-GPS), a laser range finder, a Forward Looking Infrared (FLIR) camera, and a Visible and Near Infrared (VNIR) field spectrometer.

Data from half-kilometer radial transects (from crater rims into near field ejecta) were used for topographic mapping and detailed surface classification. Sites were established at 50 meter intervals along the transects, photographed, and classified in 2 meter by 2 meter gridded zones according to lithologic size and composition. Samples of surficial fines and small blocks were collected for laboratory based spectral analyses and comparison to remote sensing image data. Vegetation data were also classified and quantified at each study zone for spectral removal [11-12].

Remote Sensing Data: Datasets from four instruments were analyzed and compared to the field data. The instruments were selected for their spectral range and resolution similarities to current Mars datasets. Detailed specifications are available in previous work [1-2, 10]; brief descriptions follow.

IKONOS is a 4 band VNIR satellite based imager with 1m spatial resolution, chosen for its similarity to both the Mars Orbiter Camera (MOC) and High Resolution Imaging Science Experiment (HiRISE). Hyperion and the Airborne Visible/Infrared Imaging Spectrometer (AVIRIS) are hyperspectral instruments that image in the VNIR and short wave infrared (SWIR) spectral range, selected for their similarity to the Compact Reconnaissance Imaging Spectrometer (CRISM). The Advanced Spaceborne Thermal Emission and Reflection Radiometer (ASTER) is a multispectral VNIR, SWIR, and TIR instrument that was chosen because it correlates well with data from the Thermal Emission Imaging System (THEMIS) and the Mars Orbiter Laser Altimeter (MOLA). IKONOS, Hyperion/AVIRIS (AVIRIS for Meteor Crater only), and ASTER data have been now been collected and analyzed over both craters using several different approaches. Of these, results from high resolution mapping and apparent thermal inertia investigations are presented here.

Results: Using IKONOS data, ejecta has been mapped based on visible characteristics that are supported by field observations [10]. Classifications for the lithologic, ejecta, and erosional units were established based on surficial characteristics either unique to each crater or common to both. For example, lava flows are present at only El Elegante Crater, whereas large blocks are present, and can be seen in the image data, near the rims of both craters. Once identified and mapped, these zones have been compared to existing geologic maps of the craters [3-4] to determine if and how specific lithologic units are identifiable at 1m remotely sensed spatial resolution.

Mapped ejecta zones coincide relatively well with geologic maps of the craters [3-4]; however, sub-

classifications of erosional features within given lithologic units, such as fluvial gullies, are larger and more readily distinguised in El Elegate's ejecta blanket (Fig. 1). This is indicative of a wetter climate history, supported by the presence of more than double the vegetation, by areal coverge, observed at El Elegante compared to Meteor Crater [10].

IKONOS comparisons of the ejecta blankets show that ejecta deposits at El Elegante have greater variability further from the crater rim than those at Meteor Crater. This variability includes more pronounced fluvial erosion features; Meteor Crater ejecta shows evidence for pronounced aeolian resedimentation.

In addition to high resolution mapping using IKONOS, apparent thermal inertia data have been generated utilizing coregistered ASTER day and night TIR images in conjunction with VNIR data. This analysis was performed to validate field observations of different block size patterns observed in the volcanic and impact environments [10]. From field classifications, block size, block abundances, and fines abundances were recorded and subsequently compared. El Elegante Crater had larger blocks more distally distributed along transects than Meteor Crater.

Apparent thermal inertia calculations confirm higher values within the ejecta blanket of El Elegante, closer in value to the coherent wall rock of the interior of the crater, than the apparent thermal inertia values observed at Meteor Crater (Fig. 2). This implies larger and more abundant blocks throughout El Elegante's near field ejecta. Although the ejecta size classifications established during the field campaigns are beyond the detection of even the highest resolution remote dataset utilized, the relative block sizes and abundances for each crater can be inferred through thermal inertia [13-14].

An important consideration in an attempt to constrain the association of block size to crater formation process is the higher resistance to fracturing and subsequent weathering of El Elegante's target rock. How this affects overall block size in the present day ejecta field is still under consideration and is one subject of continuing work.

References: [1] Peet, V.M. et al. (2005), *LPS XXXVI,* Abstract #2080. [2] Ramsey, M.S. and D.A. Crown (2004), *LPS XXXV,* Abstract #2031. [3] Hartmann, W.K. and G. Neukum (2001) *Space Science Reviews 96*: 165-194. [4] Gutman, J.T. (1976) *GSA Bull., 87*, 1718-1729. [5] Greeley R. et al. (1985) *NASA Con. Rep. 177356*, 44 pp. [6] Gutman, J.T. (2006) *GSA Annual Meeting, Paper 14-3.* [7] Shoemaker E.M. (1960) *Princeton Univ. Press*, 55 pp. [8] Ramsey M.S. (2002) *JGR, 107*, doi:10.1029/2001JE001827. [9] Wright S.P. and M.S. Ramsey (2006) *JGR, 111*, doi:10.1029/2005JE002472. [10] Peet V.M. et al. (2006), *LPS #XXXVII*, Abstract #2323. [11] Hurcom S.J. and A. R. Harrison (1998) *Int. J. Rem. Sens., 19,* doi:10.1080/014311698214217. [12] Clark, R. N. (1999), *Chapter 1: Manual of Remote Sensing, Volume 3*, RS for the Earth Sci, (A.N. Rencz, ed.) p 3- 58. [13] Christensen, P.R., (1982) *JGR, 87,* 9985-9998. [14] Edgett, K.S. and P.R. Christensen (1991) *JGR 96*, 9622765E.

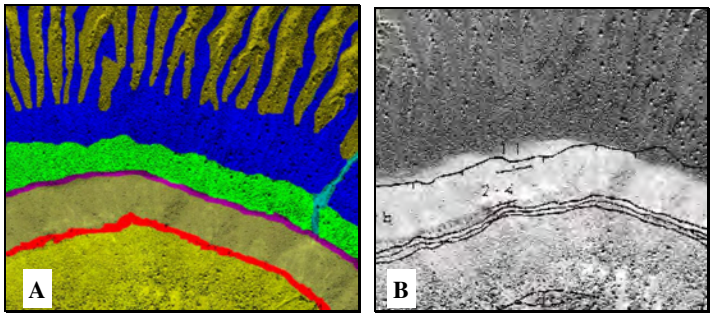

Figure 1: IKONOS data of the northern crater rim and near field ejecta of El Elegante Crater. **(A)** Classification image showing the crater rim in purple and eroded gullies as a deep yellow. This classification allows for aerial quantification of surficial units, which can reveal sediment transport and weathering histories. Note that thin basalt layers in the crater wall rock identified in established geologic map [4] from Figure 1B are not readily discernable as separate layers and are grouped as a single layer (red). **(B)** Geologic map overlay [4] warped from selected ground control points. Note that gullies and near rim blocky ejecta are not specifically identified.

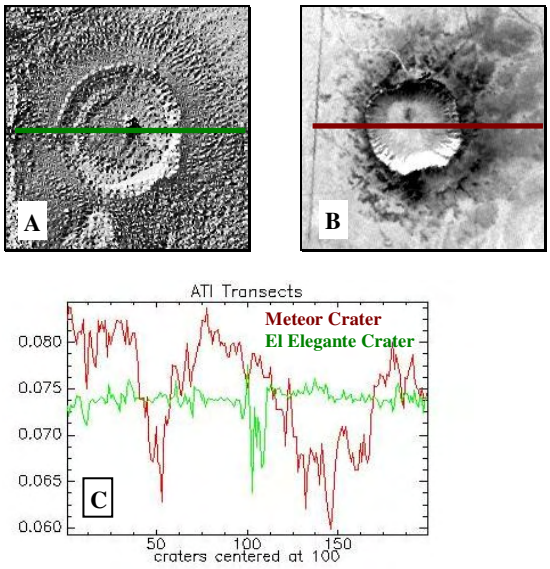

Figure 2: Apparent thermal inertia (ATI) data. **(A)** El Elegante Crater. **(B)** Meteor Crater. **(C)** Plot of ATI values for east to west transects across both images. Lower values coincide with darker (lower ATI) values in the images.